International Journal for Housing Science and Its Applications
Publish August 10, 2025. Volume 46, Issue 4 Pages 3547-3562

https://doi.org/10.70517/ijhsa464483a

Real-Time Monitoring and Data Analysis of Geotechnical Behavior in Underground Engineering Construction

Jianwei Shen[1], Xulong Duan[1,*], Fang He[1], Xiuping Zhang[1] and Na Na[1]
[1] School of Urban Construction, Yunnan Open University, Kunming, Yunnan, 650500, China
Corresponding authors: (e-mail: pkudxl0007@163.com).

Abstract This paper focuses on the evolution of geotechnical behavior of building foundations during underground engineering construction. Combined with the actual underground engineering construction situation and civil engineering professional knowledge, it defines several common geotechnical behavior parameters and characteristics during construction. Using high-precision automatic sensors to collect real-time dynamic data in the construction project, combining genetic algorithm and support vector mechanism to build real-time early warning and monitoring model, and analyzing the application of this method in the regulation of underground construction project and the change of geotechnical behaviors through examples.The distribution of displacement changes in geotechnical behaviors from June to November ranges from 0 to 13/mm, and the maximum relative error of prediction reaches 0.083, with the overall displacement prediction error is 0.084%. In addition, as the discount factor increases, it leads to a larger increment of displacement and deformation in the geotechnical behavior, which reveals that the peripheral rock destabilized parts of the underground construction should be strengthened to be monitored during the construction process. The analysis of geotechnical behavior makes the construction and long-term use of the building safety is guaranteed, and promotes the sustainable development of economic and social effects.

Index Terms underground engineering construction, geotechnical behavior, civil engineering, genetic algorithm, support vector machine

I. Introduction

Rock mechanics is the use of mechanical principles and methods to study the mechanics of rocks and mechanics-related phenomena of an emerging science, is a recent development of a strong application and practice of emerging disciplines and fringe disciplines, the scope of its application involves mining, civil construction, water conservancy and hydroelectricity, railroads, highways, geology, earthquakes, petroleum, underground engineering, marine engineering, and so on, many of the rock engineering related engineering fields [1]-[4]. It is not only closely related to national economic infrastructure, resource development, environmental protection, disaster mitigation and prevention, with important practical value, but also a basic discipline combining mechanics and geology [5].

With the increase of the world population density and the progress of urban and rural construction, the building structure has been developed in the direction of high-rise structure and underground structure, underground space as an important natural resource to be developed and utilized in the construction of the national economy has been more and more to show its strong economic and social benefits. The Chinese people have a long history of development and utilization of underground engineering [6]-[8]. As early as hundreds of thousands of years ago, Beijing apes have been using Zhoukoudian natural cave as a shelter, as far back as the ancient times, our ancestors have built all over the northwest of the loess kiln caves and magnificent underground mausoleums. After the founding of new China, all kinds of underground construction has been a very large-scale development, such as railroad and highway tunnels, underground hydroelectric power stations and all kinds of hydraulic tunnels, mine shafts and alleys, national defense and people's air defense projects, urban subway and river tunnels, underground commercial streets and underground garages and so on. At the same time, the theory of geotechnical mechanics and underground structure design and calculation is also progressing and improving [9], [10].

Ensuring production safety and reducing project costs are the main tasks of geotechnical research. In order to do so, it is necessary to carry out scientific preliminary design on the basis of geological exploration. However, due to the complexity of the geotechnical medium, many aspects of the work still rely mainly on empirical methods. That is, the engineering analogy method is mainly. In the actual construction process, through the qualitative observation of some geotechnical phenomena, some behavioral characteristics of geotechnical media can be obtained, and then form the experience in the minds of engineers [11], [12]. However, the experience is only a qualitative summary

of typical projects in the past, which cannot fully reflect the nature of geotechnical behavior. Moreover, each geotechnical and underground engineering project has its own characteristics, which makes the empirical method cannot make a scientific decision in some aspects. Thus, for the sake of production safety, it is necessary to increase the cost of the project as a price [13]-[15].

With the rapid development of computers, so that still follow the theory of solid mechanics as the basis, numerical methods as a means of finite element method to solve complex boundary value problems possible, thus greatly expanding the scope of application of the finite element method, soon to become the main means of geotechnical analysis [16], [17]. With the combination of geotechnical new results of the corresponding research, as well as the means of more perfect, the connotation of the method is richer. However, it was soon found that the finite unit method did not solve the problem of low reliability of theoretical analysis. Some people call the finite unit method as parametric simulation, that the results of the calculation and the actual situation is a big difference, mainly because the parameters are not allowed to give. In fact, this is only one aspect of the problem [18], [19]. If the boundary conditions, geometric equations, equilibrium equations are basically in line with the objective reality, the geotechnical materials, which have a great influence on the calculation results, are given with a considerable degree of blindness, which not only reflects that the study of the real geotechnical model is not yet perfect, but also involves a variety of assumptions for the selection of the constitutive model [20], [21]. Therefore, in order to further improve the reliability of the calculation, it is necessary to solve the input geotechnical property parameters and their constitutive models, which are the two major frontier topics of the current geotechnical research.

This topic is different from the traditional geotechnical behavior research in underground engineering construction, but the machine intelligence algorithm is perfectly integrated into the traditional geotechnical behavior research in underground engineering construction, in order to achieve the purpose of real-time dynamic monitoring, and to provide safety for the underground engineering construction as the most important innovation point of this topic. Geotechnics is introduced into underground engineering construction and underground engineering construction program is developed. The parameters and variables required for monitoring and analyzing the geotechnical behavior during construction are defined, and the calculation formulas for the parameters are also given. Subsequently, a high-precision automatic sensor is used to acquire the research data, and a support vector machine based on genetic algorithm optimization is proposed to realize real-time dynamic monitoring and analysis of geotechnical behavior in underground engineering construction, and to solve the characteristic of the acquired data with temporal changes. Combined with the parameters of geotechnical behavior, it confirms that this paper constructs the detection model, and tests the practicality of the monitoring model of this paper according to the displacement monitoring, deformation early warning analysis, and dynamic monitoring and warning in the geotechnical behavior.

II. Theoretical Foundations

II. A. Definition of geotechnics and its applications

II. A. 1) Definition of geotechnics

The theory and methods of design calculations for underground structures are based on the discipline of geotechnics. Here, a little bit about geotechnical aspects is introduced first. The research object of geotechnics is the multi-phase (solid, liquid, gas) anisotropic pore (fissure) geotechnical body [22]. The expression of geotechnics in geotechnical and subsurface engineering is closely related to the geological conditions, and also has a complementary influence on factors such as the type of project, construction process, support method and time.

II. A. 2) Geotechnical applications

Geotechnical inverse problem is relative to the positive problem, is based on the field measurement of the physical and mechanical properties of geotechnical body inverse parameters or a means of its intrinsic model, which is not purely a mechanical solution process, but also contains a system control and optimization techniques. Therefore, the result of the inverse problem is an “equivalent parameter” or “equivalent model” that takes into account the physical properties of the system and increases the principles of fit and simplicity. Although the meaning of this result is a little vague, but its practical value is to make the positive analysis of the results of the credibility of the greatly increased, which is exactly what the actual engineering needs.

II. B.2.2 Underground construction program

Although many scholars have explored the construction technology of underground engineering room, but different underground engineering room structure construction program, construction characteristics of the difference is large, so there is the underground engineering construction safety problems described in the previous article, this paper to the traditional building as the background, put forward the underground engineering construction program, not only a detailed analysis of the common underground engineering construction program, and at the same time, for

the following real-time geotechnical behavior in underground engineering construction At the same time, it lays the theoretical foundation for real-time monitoring and analysis of geotechnical behavior in underground engineering construction.

II. B. 1) Basement foundation formwork construction

The side slab of underground project adopts multi-layer plywood template, supported by steel pipe fasteners or wooden throw braces, square wood for cross flute, steel pipe for grill, and tensile bolts for pulling support in the wall slab, and brick tire mold for foundation beam and bearing platform. Before supporting the mold of basement side slab, the center line and side line of the wall are put on the bedding first, the template of one side is erected and lifted straight with a wire hammer, and then the back flute and support are installed and fixed after correction. After that, reinforcement bars were tied, and after the protective layer of reinforcement bars and internal bracing iron between reinforcement bars were installed, the other side of the template was supported, and external support was added to prevent the template from going out of the way, and the bottom of the template was left with a sweeping opening for removing garbage. The base structure has high requirements for waterproofing, when the template is installed, the steel wires and bolts for fixing the template should avoid contacting the inside of the template to prevent the steel wires, bolts and cleats from intruding into the area of the base structure, thus affecting the external dimensions of the base template and leading to a reduction in the waterproofing level of the underground concrete when the concrete is poured, affecting the waterproofing. When the template fixing needs to be bolted, it needs to be equipped with a water stop ring between the bolt and the template, and the water stop ring and the bolt should maintain a tight connection between the bolt and the template is firmly installed. Before the construction of underground engineering foundation beams, the position of the brick mold needs to be accurately placed. The offset of the position of the brick mold will seriously affect the size and linearity of the foundation beam, so it is necessary to put out the centerline of the foundation beam during the construction of the brick mold, and lay the brick mold according to the centerline position. Requirements for brick wall masonry must be firm, in order to prevent the lateral pressure generated during the pouring of concrete caused by the displacement of the brick mold, the formation of foundation bending and other defects. Pre-embedded parts and pre-drilled holes should not be missed, and the installation must be firm and accurate position. After the completion of the brick mold, the project department timely conducts quality inspection and technical review of the project.

II. B. 2) Basement foundation reinforcement construction

Reinforcing steel fabrication and welding are the same as the main project fabrication and welding requirements. Due to more and dense foundation reinforcement, the foundation main reinforcement is connected by double-sided welding. Before the construction of foundation reinforcement, the foundation is leveled, and according to the leveling of the foundation, the leveling of the bedding layer is achieved through bedding construction.

Support frame structure as shown in Figure 1, support frame structure layer reinforcement due to the bracket fixed, can ensure that no displacement, support frame set spacing control in 1 m. Spacing is too small to affect the overall structural reinforcement rate, spacing is too large can not play a supporting role.

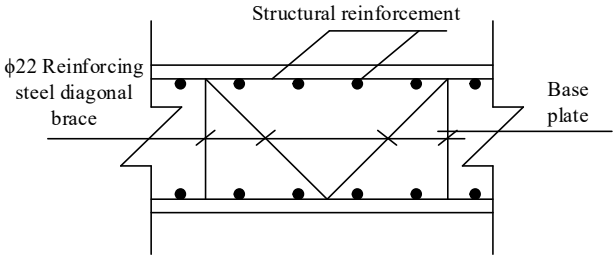

Figure 1: Support structure

The schematic diagram of rebar insertion and positioning is shown in Figure 2. The reinforcement of the foundation beam and the structural column reinforcement of the underground engineering cross part, the structural column reinforcement extends out of the reinforcement of the foundation beam, and the excessive length of the reinforcement is deflected under the action of self-weight, which will drive the foundation reinforcement to be deflected, so use the locating hoops to tie and fix the structural column along the inner edge, so as to make the structural column reinforcement keep upright. At the same time, temporary diagonal support is arranged and fixed between the structural column and the foundation reinforcement, so that the foundation reinforcement and the structural column reinforcement form a temporary stable triangular state to avoid the offset of both reinforcement.

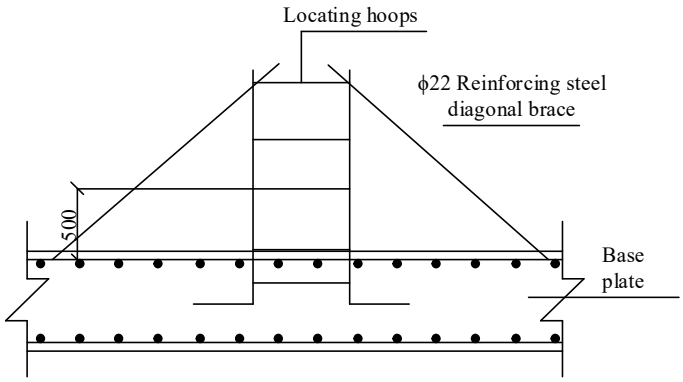

Figure 2: Positioning diagram of interpolation

II. B. 3) Basement foundation concrete construction

Before the concrete is poured, the stability of the reinforcement and formwork needs to be checked and needs to be determined by the supervising engineer. The temporary support stability is checked, the gaps inside the formwork are cleaned, and the formwork is kept in a wet condition before pouring. When pouring concrete, the bottom slab of the underground building, then the wall panel of the underground building, and the top slab wall are poured in accordance with the principle of pouring in layers, first low and then high. In order to ensure the compactness of concrete, the concrete of the base plate is poured by catching slurry method. Bearing platform surface and foundation beam, the upper surface of the plate in a timely manner with a wooden trowel smoothing, is strictly prohibited prematurely on. After the concrete pouring is completed, even if the water sprinkling maintenance, maintenance time to ensure that more than 14 days, to ensure that the concrete structure is moist.

III. Geotechnical behavior monitoring in underground engineering construction

III. A. Geotechnical behavior and deformation mechanical properties

Geotechnical soils are highly heterogeneous and anisotropic media cut by many discontinuous structural surfaces such as fault joint levels. There is an urgent need for a clear understanding of their mechanical properties for monitoring the mechanical behavior of geotechnical soils in underground construction. In order to determine the mechanical behavior of geotechnical or its should be used in the relevant calculation parameters, and at the same time to carry out the necessary analytical calculations. Because the mechanical behavior of geotechnical properties is very complex, it should be said that the calculation theory and method about discontinuous rock mass is not very mature, and more assumptions have to be made. The following describes the deformation mechanical properties of intact rock masses and jointed fissures, respectively:

III. A. 1) Geotechnical behavior during construction

Figure 3 represents typical curves of geotechnical behavior in underground construction, which are roughly divided into five regions. The specific descriptions are as follows:

(1) Compaction stage (OA)

The specimen is pressurized, the cracks are closed, and the curve is slightly nonlinearly concave $\left(\frac{d^2\sigma}{d\varepsilon^2}>0\right)$ and locally slightly cracked. This is due to the original pores and cracks in the rock is gradually pressed tightly closed phenomenon, for dense rock this region is not or very small, A points named initial compaction.

(2) Elastic phase (AB)

$\sigma\sim\varepsilon$ The curve grows in a straight line, and in the region of I and II, if the load is removed and the deformation is fully recovered, the stress value corresponding to point B is called the elastic limit or yield stress, which marks the end of the elastic deformation and the beginning of the stabilizing fracture propagation.

(3) Nonlinear phase (BC)

$\sigma\sim\varepsilon$ The curve is nonlinearly upconvex $\left(\frac{d^2\sigma}{d\varepsilon^2}<0\right)$ and the stable fissure propagation develops to unstable propagation, which is accompanied by many microfractures accordingly, and the rock mass enters into the yielding state (plastic deformation is generated), and the volume expands.

In region III, when the load is removed at any point P, the stress-strain will decrease along the line PQ, and the rock has a residual plastic strain as the compressive stress drops to zero. That is, after the stress exceeds the

elastic limit, e.g. at point P, the corresponding strain can be considered as consisting of an elastic strain portion (QS) and a plastic strain portion (OQ). If reloaded from point Q, the stress-strain will rise along QR to point R, reconnecting with lines BC. The proximity of PQ and QR to the parallel AB line corresponds to an increase of the elastic limit from the value of stress corresponding to point B to the value of stress corresponding to point R, i.e., the phenomenon of strain-hardening or work-hardening occurs, and the value of compressive stress corresponding to point C is called the compressive strength.

(4) Rupture stage (CD)

The bearing capacity of the specimen decreases significantly, the $\sigma \sim \varepsilon$ curve begins to decline rapidly, the crack continues to expand, the specimen appears to shear expansion (expansion), the curve undulates, gradually to a smooth, to reach the residual strength. The strength of the rock gradually decreases in the CD section, strain softening phenomenon occurs, and the D point represents the residual strength.

In the I, II, III region of deformation, with the deformation increases the stress also increases, i.e., $d\sigma \cdot d\varepsilon > 0$, known as the stable stage: in the IV region of deformation, with the deformation increases the stress decreases, i.e., $d\sigma \cdot d\varepsilon < 0$, known as the non-stable stage. As a result of plastic deformation, the slope of the unloading curve is reduced, i.e., elastic-plastic coupling occurs, and this phenomenon is more significant in the unsteady stage.

(5) Tensile stage (OE)

The $\sigma \sim \varepsilon$ curve under tensile stress approximates a straight line, and when the tensile stress reaches the tensile strength of the rock, the rock is cracked and destroyed, the strength is reduced to zero, and there is a great increase in deformation.

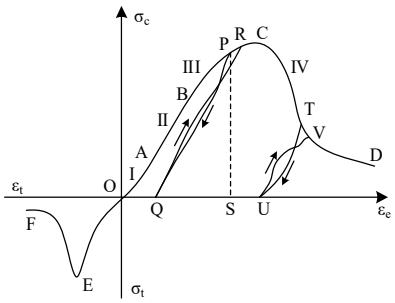

Figure 3: Geotechnical behavior curve

III. A. 2) Mechanical Behavioral Properties of Nodal Fractures

The deformation of the fissure is mainly normal deformation and tangential deformation as well as the coupling between the two, the earliest stress-strain curve was used to study the deformation behavior of the fissure, the normal stiffness K_n and shear stiffness K_s were introduced to describe the relationship between the normal stress σ_n and the normal displacement V, as well as the relationship between the shear stress τ and shear displacement d_h, and nodal units were used to simulate.

(1) Deformation characteristics of nodal fissures

The typical normal deformation curve of the fracture is shown in Fig. 4(a), and there is a very obvious nonlinear relationship between normal stress and normal displacement. Many scholars have studied this nonlinear behavior, among which the more widely cited is the Bandis fissure model:

$$\Delta V_j = \frac{\sigma_n}{k_{n_0} + \sigma_n V_m} \tag{1}$$

where, k_{n_n} is the initial normal stiffness, V_m is the initial mechanical gap width, i.e., the maximum closure It is considered that the maximum closure of the fissure V_m should be less than the thickness of its rough body a_j (also known as the maximum gap width of the fissure), and σ_n is the normal stress at the fissure surface, where k_{n_0} and V_m are related to the initial stress state. The normal stiffness K_n of the fissure can be obtained from equation (2) as:

$$K_n = \frac{\partial \sigma_n}{\partial \Delta V_j} = k_{n_0}\left[1 - \frac{\sigma_n}{V_m k_{n_0} + \sigma_n}\right]^{-2} \tag{2}$$

(2) Shear deformation characteristics

The relationship between typical fissure shear deformation and shear stress is shown in Fig. 4(b). The shear deformation curve can be divided into three stages: pre-peak, peak, and post-peak, and exhibits an obvious nonlinear behavior, with a very complex strain softening behavior after the peak. The relationship between the pre-peak shear stress τ and shear deformation τ_1 can generally be fitted by a hyperbola:

$$\tau = \frac{u}{m + nu} \tag{3}$$

where τ is the forward shear stress, u is the tangential displacement, m, n are constants related to σ_n.

An empirical formula for the shear stiffness is presented considering the structural face size effect:

$$K_s = \frac{100}{L}\sigma_n \tan\left[JRC \cdot \lg\left(\frac{JCS}{\sigma_n}\right) + \varphi_r\right] \tag{4}$$

where σ_n is the normal stress, φ_r is the residual friction angle, JRC is the nodal roughness coefficient, JCS is the compressive strength of the nodal surface, and L is the length of the fissure, reflecting the effect of size effect on K_s. The shear stiffness K_s of the fissure increases with increasing normal stress σ_n. The shear deformation of the fissure is usually accompanied by shear expansion or shear contraction, as shown in Fig. 4(c). The deformation properties of rock nodal fissures are controlled by their unit stiffness in compression and in shear and their strength. The nodal normal stiffness K_n depends on: the solid-to-solid contact area between the two nodal surfaces, the shape of the interstitial space, and the characteristics of the filling material. Whereas, the tangential stiffness K_s depends on: roughness, shape of the interstitial space, and characteristics of the filling material. In addition, the stiffness of the nodal fissure is also affected by humidity, which affects the variation of K_n and K_s through its influence on the filling material characteristics.

It is generally believed that the ratio of K_n to K_s is in the range of 5 to 10. In practice, K_n and K_s are difficult to determine except by actual measurement, and the above rule of thumb can be further explored in practice.

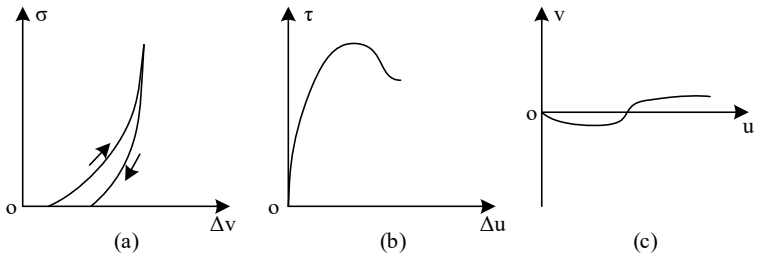

Figure 4: The stress of the joint is a relative displacement curve

(3) Shear strength properties of jointed fissures

The damage of jointed rock body is dominated by the damage along the joint surface, thus, the peak shear strength of the joints becomes the most important mechanical property of the jointed rock body, and has been one of the most important research topics in geotechnics. There are two ways to study the peak shear strength of rock and soil. The shear and shear expansion properties of the raised body are related to the normal stress, and the following empirical equations for the shear strength of joints are proposed:

$$\tau = \sigma \tan\left[JRC \cdot \lg\left(\frac{JCS}{\sigma}\right) + \varphi_b\right] \tag{5}$$

where JRC is the joint roughness coefficient, JCS is the compressive strength of the joint surface, σ is the normal positive stress, and φ_b is the basic friction angle of the joint.

III. B. Construction of real-time construction monitoring model

Effective selection of geotechnical parameters is an important factor in determining the accuracy of the monitoring results, the establishment of the model is often simplified to a certain extent on the basis of the actual situation, in order to get closer to the construction monitoring data, this paper adopts high-precision automatic sensors to obtain the research data, due to the acquired data has a temporal change characteristics, the proposed genetic algorithm based optimization of the support vector machine, to achieve the underground This paper adopts high-precision automatic sensors to obtain research data, and proposes support vector machine optimized based on genetic algorithm to realize real-time monitoring and data analysis of geotechnical behavior in underground construction. The detailed principle and process are as follows:

III. B. 1) Data acquisition

The main components of the data acquisition system are various types of high-precision automatic sensors. At present, these sensors are an important part of the composition of the automatic monitoring system, and they can realize the sensing and acquisition of a variety of test items, and they have a number of functions, such as high precision, high integration and wireless intelligent sensing, which makes the underground sensing network gradually realize automation and intelligence.

The contents of data collection include: normal stiffness, shear stiffness, normal stress, shear stress, tangential displacement, normal displacement, friction angle, etc. It is evident that compared with the traditional monitoring methods, the contents and objects of data collection of this new monitoring system are not very different. However, due to the use of automatic sensors, the monitoring efficiency is greatly improved, and massive data from multiple sources can be collected at the same time.

III. B. 2) Genetic Algorithm Theory

Classical genetic algorithm (GA) belongs to a kind of evolutionary algorithm. It is based on Darwin's theory of biological evolution “survival of the fittest, survival of the fittest” [23]. The execution process of the genetic algorithm mimics the complete process of biological evolution in nature, which is a relatively robust, stochastic and adaptive optimization process. The classical genetic algorithm needs to generate an initial population according to the problem before starting the operation, and each individual (chromosome) in the population is coded to execute the evolutionary strategy, and after several evolutions, the individual with the highest fitness is selected, which is the optimal solution of the problem.

(1) Coding method

Coding is the basis of classical genetic algorithm. Genetic algorithms can not directly take operations on the solution of the problem, which needs to be encoded and transformed into individuals (chromosomes) that can be handled by genetic algorithms.

The encoding methods used by classical genetic algorithms are usually the following three:

(a) Floating point method: this method encodes individual genes using floating point (real) numbers, i.e., each gene is a floating point number and the length of the chromosome is determined by the number of genes it contains. The floating point method has some advantages in solving optimization problems where the parameters are continuous variables.

(b) Binary method: This method uses “0” and “1” to encode the gene bits, and each chromosome is a string of binary symbols. The binary method is the most common and frequently used encoding method in classical genetic algorithms.

(c) Gray code: Gray code also uses “0” and “1” for encoding, but unlike binary code, only one bit is different between two consecutive integers corresponding to Gray code. The Gray code method can enhance the search ability of classical genetic algorithm.

(2) Initial population selection

Before starting the genetic operation it is necessary to set the population size and generate the initial population. The execution of the genetic algorithm depends on the selection of the initial population, so it is very critical to set the population size reasonably and select the initial population. The larger the population, the higher the diversity of the population and the less likely the algorithm will fall into the local optimum, but the larger the population, the higher the computational cost and easy to mature prematurely. At the same time, the selection of individuals in the population also affects the execution ability of the algorithm. If the individuals in the population are clustered near the optimal solution, then the algorithm converges quickly, and vice versa, the convergence rate is slower. Therefore, when selecting the initial population, the individuals should be uniformly selected in the estimated solution space to ensure the execution efficiency of the algorithm.

(3) Adaptation function

The function of the fitness function is to determine an individual's ability to adapt to the environment. According to the evolutionary theory of “survival of the fittest”, the higher the degree of adaptation of an individual, the stronger its adaptive ability and the less likely to be eliminated. The individual with the highest fitness value is the optimal solution of the optimization problem. The fitness function $F(x)$ is usually selected in the following three ways:

(a) The objective function $f(x)$ of the optimization problem is chosen as the fitness function:

If the objective function $f(x)$ is a maximization problem, then there are:

$$F(x) = f(x) \tag{6}$$

If the objective function $f(x)$ is a minimization problem, then there is:

$$F(x) = -f(x) \tag{7}$$

(b) Boundary construction method:

If the objective function $f(x)$ is a maximization problem, we have:

$$F(x) = \begin{cases} f(x) - c & f(x) - c > 0 \\ 0 & f(x) - c \le 0 \end{cases} \tag{8}$$

where c is a suitably large positive number.

If the objective function $f(x)$ is a minimization problem, we have:

$$F(x) = \begin{cases} c - f(x) & f(x) - c > 0 \\ 0 & f(x) - c \le 0 \end{cases} \tag{9}$$

where c is a suitably large positive number.

(c) Conservative estimation methods:

If the objective function $f(x)$ is a maximization problem, we have:

$$F(f(x)) = \frac{1}{1 + c + f(x)} \tag{10}$$

where $c \ge 0$, $c + f(x) \ge 0$.

If the objective function $f(x)$ is a minimization problem, we have:

$$F(f(x)) = \frac{1}{1 + c - f(x)} \tag{11}$$

where $c \ge 0$, $c - f(x) \ge 0$.

The fitness function is often not static. Because in the primary stage of the algorithm, in order to prevent the phenomenon of premature maturation, the difference between individuals needs to be appropriately reduced, while in the late stage of the algorithm, in order to accelerate the rate of convergence, the gap between individuals needs to be increased. Therefore, the fitness function needs to be changed accordingly to the actual situation in order to make the algorithm achieve better results.

(4) Genetic operator

The core of the classical genetic algorithm is to generate a new population by imitating the genetic operation of biology, which contains three kinds of genetic operations: selection, crossover and mutation.

(a) Selection

The general selection step is if the size of the population is N and the fitness of individual i is written as $F(i)$, then the probability p_i that individual i is selected can be written:

$$p_i = \frac{F(i)}{\sum_{i=1}^{N} F(i)} \tag{12}$$

Construct a roulette wheel with all the individuals in a certain order according to their probabilities, and randomly generate a value in the interval $[0,1]$. The individual whose probability interval the value belongs to is selected for the next generation. Repeat this step until a new generation of the population is selected.

(b) Crossover operator

The crossover operation reflects genetic recombination in biology. In nature, the genetic recombination of individuals of the parent generation through mating to produce offspring is the most important part of the reproduction process. Therefore, for the classical genetic algorithm designed in imitation of biology, the crossover operation is also a necessary condition for generating new individuals.

(c) Mutation operator

The mutation operation embodies the gene mutation in biological evolution. Organisms in nature may generate new genes or change the original genes after gene mutation. For classical genetic algorithms, mutation operation can maintain the diversity of the population, and at the same time, it can strengthen its searching ability and prevent premature maturation. Therefore, the crossover operator and mutation operator are used together, which can make the classical genetic algorithm faster and better to find the optimal solution of the problem.

(5) Termination condition

The termination condition of the genetic algorithm needs to be triggered when the genetic algorithm finds the optimal solution or no longer evolves. There are two most commonly used termination methods:

(a) Setting the maximum number of iterations of the population: before the execution of the algorithm, estimate the number of iterations needed to find the optimal solution, set the maximum number of iterations, and trigger the termination condition when the population of the genetic algorithm has evolved to the pre-determined maximum number of iterations, and the solution obtained by the individual with the highest adaptability in the final generation is the optimal solution found.

(b) Setting a threshold value: when the change in the fitness of individuals in consecutive generations is less than the threshold value, the population is considered to have completed evolution, and the solution corresponding to the individual with the highest fitness in the final generation is the optimal solution found.

III. B. 3) Support vector machine theory

Support vector machines provide a feasible tool for dealing with nonlinear problems and are highly flexible and useful for complex nonlinear dynamic systems [24]. Compared to other machine learning algorithms, support vector machines are able to be highly adaptable to data samples and are suitable for analyzing small sample data. The goal of the support vector machine algorithm is to find the optimal hyperplane. This plane is able to divide the data samples into two classes and maximize the distance between this plane and the two classes.

Let the number of dataset of samples be: $\left\{\left(x_i, y,\right) \mid x, R^p, y_i \in \{-1,1\}, i=1,2,\ldots,n\right\}$, where n denotes the number of samples, x_i denotes the input vector, and y_i denotes the data classification label. When the data sample points are linearly divisible, a hyperplane can be found in the feature space, which can be expressed as Eq:

$$w \cdot x_i + b = 0 \tag{13}$$

In order to classify all samples correctly, the following optimization problem can be written:

$$\begin{cases} \min \varphi(x) = \dfrac{1}{2}\|\omega\|^2 + C\sum\limits_{i=1}^{t} \xi_i \\ s.t. y_i\left(\omega \cdot x_i + b\right) \geq 1 - \xi_i, \xi_i \geq 0, i = 1,2,\ldots,N \end{cases} \tag{14}$$

Where: ξ_i is the relaxation variable. C is the penalization factor. b is the offset.

Due to the linear indivisibility of bearing fault classification, the input samples are nonlinearly mapped to a high-dimensional eigenvector space, the optimal hyperplane is constructed, and the Lagrange function is introduced, which is transformed into a dyadic problem according to the strong dyadic nature of convex optimization:

$$\begin{cases} \min L(\omega, b, i) = -\dfrac{1}{2}\sum\limits_{,j=1}^{N} \lambda\lambda_i, y_i y_i K\left(x_i \cdot x_j\right) + \sum\limits_{i=1}^{N} \lambda \\ s\lambda. \sum\limits_{i=1}^{N} \lambda y_i = 0, \lambda \geq 0, i = 1,2,\ldots,N \end{cases} \tag{15}$$

Then the final categorical hyperplane is:

$$f(x)=\operatorname{sgn}\left\{\sum_{i,j-1}^{n}\lambda_i y_i K\left(x_i,x_j\right)+b\right\} \tag{16}$$

where, $K\left(x_i,x_j\right)$ is the kernel function, generally, there are several common kernel functions:

Linear kernel function:

$$K\left(x_i\cdot x_j\right)=x^T\cdot x_i \tag{17}$$

Radial basis kernel function:

$$K\left(x_i\cdot x_j\right)=\exp\left\{g\left|x\cdot x_i\right|^2\right\},g>0 \tag{18}$$

Polynomial kernel functions:

$$K\left(x_i\cdot x_j\right)=\left(gx^T\cdot x_i+1\right)^q,g>0,q>0 \tag{19}$$

Sigmoid kernel function:

$$K\left(x_j\cdot x_j\right)=\tanh\left(\beta x^T x_j+\theta\right),\beta>0,\theta<0 \tag{20}$$

III. B. 4) Mathematical modeling

The mapping relationship between rock mechanical parameters and rock displacements is expressed using support vector machines, as shown in Eqs. (21) and (22):

$$SVM\left(x_1,x_2,\cdots,x_n\right) \tag{21}$$

$$\begin{cases}SVM\left(X\right):R^n\rightarrow R\\ Y=SVM\left(X\right)\\ X=\left(x_1,x_2,\cdots,x_n\right)\end{cases} \tag{22}$$

where $X=\left(x_1,x_2,\cdots,x_n\right)$ represents the unknown geotechnical parameters, which are normal stiffness, shear stiffness, normal stress, shear stress, tangential displacement, normal displacement, friction angle and other parameters. Y represents the key node displacements obtained from field measurements.

The establishment of a support vector machine model first needs to prepare multiple sets of data samples for the algorithm to learn and train. The type of folding coefficient and kernel function of the support vector machine has an important impact on the predictive ability and application range of the model, so the genetic algorithm is used to optimize the parameters of the support vector machine. The specific steps of geotechnical parameter inversion are as follows:

(1) Randomly select a set of parameters with a scale of N as the initial value, train the support vector machine model with the obtained sample data, and then use the obtained model to regress the known sample data for prediction, and take the maximum error value of the given detection sample as the adaptation value of the model screening sample.

(2) Genetic algorithm is used to find the optimal parameters during the model training process until a set of optimal support vector machine training parameters is obtained, so that the optimal parameters correspond to the optimal support vector machine model, and the optimal model can accurately reflect the nonlinear mapping relationship between the geotechnical parameters and geotechnical displacements.

Usually, when solving the geotechnical engineering parameter inversion problem, the displacement values of several key nodes are selected to establish a computational model, and then the sum of squares function of the measured and predicted displacements of all the key nodes should be constructed, which is utilized as the objective function, and the minimum of the sum of squares is used as the basis of the end of the parameter inversion. The ultimate goal of parameter inversion is to solve a set of rock mechanical parameters that satisfy the optimal conditions of the objective function. Thus, the objective function can be expressed according to equation (23):

$$F\left(X\right)=\sum_{i=1}^{n}\left[f_i\left(X\right)-y_i\right]^2 \tag{23}$$

where $X=(x_1,x_2,\cdots,x_n)$ represents a set of geotechnical parameters to be inverted: $f_i(X)$ is the calculated value of displacement corresponding to key node i. y_i is the measured value of displacement corresponding to key node i. n is the number of key nodes used for modeling purposes.

IV. Research and analysis of geotechnical behavior in construction

IV. A. Model validation analysis

According to the real-time feedback monitoring data from the construction site compared with the simulation data, the GA-SVM algorithm is used to find the geotechnical parameters with high accuracy in reverse direction, and the geotechnical layers mainly include the fill layer, clay layer, coarse sand layer and mudstone layer, and the transverse length, height, and the longitudinal length of the model are 65m, 50m, and 40m, respectively, taking into consideration of the influence of the boundary effect.

According to the mechanical parameters of the rock body measured at the construction site, the theoretical values of each key parameter are derived by the method of zero to whole, and Table 1 shows the value levels of each mechanical parameter. Among them, normal stiffness, shear stiffness, normal stress, shear stress, tangential displacement, normal displacement, and friction angle are the construction learning samples, and each mechanical parameter to be inverted takes five level values.

Table 1: The parameters of each mechanical parameter are evaluated

Level	1	2	3	4	5
Normal stiffness(N/m)	1.44	1.21	2.36	2.72	2.88
Shear stiffness(N/m)	1.65	1.49	1.75	1.48	1.96
Normal stress(N)	10.77	10.62	10.67	9.93	9.89
Shear stress(N)	10.42	10.92	9.68	9.95	10.71
Tangential displacement(m)	12.34	12.87	11.95	11.52	12.68
Normal displacement(m)	10.83	10.43	12.27	12.26	12.79
Friction Angle(°)	88	62	76	78	45

Taking the mudstone layer as an example, the geotechnical parameter values of the inverse extrapolation are calculated, and the specific algorithmic results are shown in Table 2.A total of 25 groups of geotechnical parameter combinations are configured according to the orthogonal test method. Sequentially, 25 groups of mechanical parameters are input into the established model, and simulation calculations are carried out in the numerical model using the original scheme, respectively, so that each group of samples consists of input values (mechanical parameters) and output values (displacement of measurement points). Twenty of these groups of data were randomly extracted as learning samples to establish the mapping relationship between rock mechanical parameters and displacements by GA-SVM machine learning algorithm, and the remaining five groups of data were used as monitoring samples.

Table 2: Specific results

Sedimentation monitoring point	Displacement direction	Numerical calculation displacement/cm	GA-SVM Estimated value	Relative error/%
1	z	9.77	9.75	0.20
2	z	10.06	10.05	0.10
3	z	10.26	10.26	0
4	z	10.19	10.33	1.37
5	z	10.26	10.28	0.19

From Table 2, it can be concluded that the GA-SVM algorithm can well establish the mapping relationship between geotechnical parameters and displacement deformation. The actual monitoring displacement values of the five measurement points are imported into the GA-SVM model for inversion of geotechnical parameters, and the geotechnical behavior parameters are shown in Table 3. It can be seen that the table contains geotechnical behavior parameters (normal stiffness, shear stiffness, normal stress, shear stress, tangential displacement, normal displacement, friction angle) of the fill, clay, coarse sand, mudstone, initial support, second lining, and reinforced area, and the geotechnical behavior data obtained from real-time monitoring at the construction excavation site are used to efficiently regress, screen, and speculate using the genetic algorithm's global search of support vector

machine algorithms to finally Realize the real-time monitoring and analysis of geotechnical behavior in underground engineering construction.

Table 3: Geotechnical behavior parameters

Name	Normal stiffness (N/m)	Shear stiffness (N/m)	Normal stress (N)	Shear stress (N)	Tangential displacement (m)	Normal displacement (m)	Friction Angle (°)
Soil packing	1.335	1.941	8.202	6.714	1.231	1.588	29
Clay	3.934	4.202	11.94	16.279	1.686	0.588	52
Coarse sand	1.025	2.778	18.972	3.819	1.937	1.635	69
Mudstone	2.052	1.814	15.282	6.515	1.045	0.268	81
Initial branch	4.649	1.518	11.971	4.303	0.158	0.729	81
Binding	3.613	3.403	17.741	6.048	1.067	0.643	55
Reinforcing zone	1.839	4.772	12.459	15.824	1.396	1.091	41

IV. B. Displacement monitoring in geotechnical behavior

IV. B. 1) Engineering overview

In this section, Case A of the underground project is selected, and the project area is overlain by the Quaternary Artificial Accumulation Layer, and underlain by the Calcareous Slate and Yanshan Stage Phyllite Layer of the Aurignacian Changlingzi Formation. Each stratum is described as follows:

Quaternary artificial accumulation layer: artificial accumulation of vegetal fill.

Aurignacian Changlingzi Formation calcareous slate: the main components are mica, quartz and calcite. Cryptocrystalline structure, plate-like structure. According to the degree of weathering, it can be divided into fully weathered rock, strongly weathered rock and medium weathered rock.

Yanshan period gabbro layer: gabbro was formed in the Mesozoic era and is a basal rock. It is produced in the form of veins and beds, generally green in color, and the main mineral components are plagioclase feldspar and pyroxene. Pyroxene structure, blocky structure. According to the degree of weathering, it can be divided into fully weathered rock, strongly weathered rock and medium weathered rock.

There are no surface streams passing through the site.

IV. B. 2) Construction monitoring data

In order to monitor the geotechnical behavior during the construction process, measurements were made by burying multi-point displacement meters on the ground, and the results of the displacement value measurements of the 4.5m deep measurement point under the surface at the mileage of DK15+605 are shown in Table 4, while the displacement changes in five different depth positions below the surface of the ground, 1.5m, 3.0m, 4.5m, 6.0m, and 7.5m were measured at the same time. The buried position is located within 50m, and a total of six multi-point displacement gauges are set up, and the displacement change values in the geotechnical behavior from June to November are distributed in the range of 0 to 13/mm.

Table 4: Construction monitoring data

Date	Value/mm	Date	Value/mm	Date	Value/mm	Date	Value/mm	Date	Value/mm	Date	Value/mm
6/30	0.12	7/25	1.73	8/18	3.92	9/11	6.73	10/6	8.92	10/30	11.06
7/1	0.32	7/26	1.81	8/19	4.16	9/12	6.94	10/7	9.09	10/31	11.11
7/2	0.33	7/27	1.83	8/20	4.21	9/13	6.96	10/8	9.16	11/1	11.22
7/3	0.34	7/28	1.84	8/21	4.27	9/14	6.99	10/9	9.20	11/2	11.27
7/4	0.51	7/29	2.27	8/22	4.44	9/15	7.33	10/10	9.21	11/3	11.31
7/5	0.68	7/30	2.31	8/23	4.52	9/16	7.51	10/11	9.22	11/4	11.41
7/6	0.71	7/31	2.33	8/24	4.52	9/17	7.54	10/12	9.27	11/5	11.43
7/7	0.76	8/1	2.37	8/25	4.56	9/18	7.62	10/13	9.32	11/6	11.48
7/8	0.89	8/2	2.38	8/26	4.62	9/19	7.63	10/14	9.43	11/7	11.65
7/9	0.90	8/3	2.46	8/27	5.03	9/20	7.65	10/15	9.55	11/8	11.68
7/10	0.93	8/4	2.47	8/28	5.04	9/21	7.76	10/16	9.60	11/9	11.70
7/11	1.03	8/5	2.52	8/29	5.13	9/22	7.83	10/17	9.67	11/10	11.70
7/12	1.06	8/6	2.56	8/30	5.23	9/23	7.85	10/18	9.93	11/11	11.93

7/13	1.10	8/7	2.59	8/31	5.28	9/24	7.87	10/19	10.06	11/12	11.98
7/14	1.13	8/8	2.68	9/1	5.43	9/25	7.91	10/20	10.16	11/13	12.01
7/16	1.18	8/9	2.72	9/2	5.65	9/26	7.93	10/21	10.30	11/14	12.04
7/17	1.21	8/10	2.92	9/3	5.74	9/27	8.26	10/22	10.39	11/15	12.04
7/18	1.22	8/11	2.95	9/4	6.06	9/28	8.38	10/23	10.41	11/16	12.09
7/19	1.30	8/12	3.00	9/5	6.20	9/30	8.45	10/24	10.48	11/17	12.13
7/20	1.45	8/13	3.16	9/6	6.23	10/1	8.50	10/25	10.56	11/18	12.43
7/21	1.49	8/14	3.64	9/7	6.41	10/2	8.58	10/26	10.62	11/19	12.53
7/22	1.56	8/15	3.67	9/8	6.43	10/3	8.76	10/27	10.67	11/20	12.71
7/23	1.61	8/16	3.77	9/9	6.55	10/4	8.87	10/28	10.87	11/21	12.71
7/24	1.62	8/17	3.87	9/10	6.69	10/5	8.89	10/29	10.91	11/22	12.76

IV. B. 3) Analysis of the effect of model displacement prediction

The results of the model displacement prediction effect analysis are shown in Table 5, where D indicates the date, A indicates the actual value, P indicates the predicted value, and E indicates the error. According to the form of the data, a single time series prediction model is used, and the prediction method adopts the method of “continuous prediction”, i.e., each prediction uses all the monitoring data before the prediction time, and each prediction uses the displacement values of 5 time nodes after the prediction. From the data recorded in the above table, it can be seen that after June 30, the displacement value has been increasing slowly until the end of November when the displacement value tends to stabilize. According to the prediction, it can be seen that the maximum relative error of prediction reaches 0.083, and the overall displacement prediction error is 0.084%, the errors are within 5%, which indicates that the geotechnical behavior monitoring method based on the genetic algorithm optimization support vector machine is practicable.

Table 5: Model displacement prediction results

D	A	P	E	D	A	P	E	D	A	P	E	D	A	P	E
6/30	0.12	0.13	0.083	8/6	2.56	2.56	0.000	9/11	6.73	6.73	0.000	10/18	9.93	9.94	0.010
7/1	0.32	0.32	0.000	8/7	2.59	2.59	0.000	9/12	6.94	6.95	0.001	10/19	10.06	10.06	0.000
7/2	0.33	0.35	0.061	8/8	2.68	2.66	0.007	9/13	6.96	6.96	0.000	10/20	10.16	10.16	0.000
7/3	0.34	0.34	0.000	8/9	2.72	2.73	0.004	9/14	6.99	7.00	0.001	10/21	10.30	10.30	0.000
7/4	0.51	0.51	0.000	8/10	2.92	2.92	0.000	9/15	7.33	7.33	0.000	10/22	10.39	10.40	0.010
7/5	0.68	0.67	0.015	8/11	2.95	2.95	0.000	9/16	7.51	7.51	0.000	10/23	10.41	10.42	0.010
7/6	0.71	0.69	0.028	8/12	3.00	2.99	0.003	9/17	7.54	7.54	0.000	10/24	10.48	10.49	0.010
7/7	0.76	0.77	0.013	8/13	3.16	3.17	0.003	9/18	7.62	7.62	0.000	10/25	10.56	10.57	0.010
7/8	0.89	0.87	0.022	8/14	3.64	3.65	0.003	9/19	7.63	7.65	0.003	10/26	10.62	10.62	0.000
7/9	0.90	0.91	0.011	8/15	3.67	3.70	0.008	9/20	7.65	7.64	0.001	10/27	10.67	10.67	0.000
7/10	0.93	0.94	0.011	8/16	3.77	3.76	0.003	9/21	7.76	7.76	0.000	10/28	10.87	10.88	0.010
7/11	1.03	1.03	0.000	8/17	3.87	3.86	0.003	9/22	7.83	7.83	0.000	10/29	10.91	10.92	0.010
7/12	1.06	1.06	0.000	8/18	3.92	3.91	0.003	9/23	7.85	7.86	0.001	10/30	11.06	11.06	0.000
7/13	1.10	1.10	0.000	8/19	4.16	4.14	0.005	9/24	7.87	7.87	0.000	10/31	11.11	11.10	0.010
7/14	1.13	1.13	0.000	8/20	4.21	4.21	0.000	9/25	7.91	7.91	0.000	11/1	11.22	11.23	0.010
7/16	1.18	1.17	0.008	8/21	4.27	4.27	0.000	9/26	7.93	7.92	0.001	11/2	11.27	11.28	0.010
7/17	1.21	1.22	0.008	8/22	4.44	4.44	0.000	9/27	8.26	8.26	0.000	11/3	11.31	11.31	0.000
7/18	1.22	1.21	0.008	8/23	4.52	4.51	0.002	9/28	8.38	8.38	0.000	11/4	11.41	11.39	0.020
7/19	1.30	1.31	0.008	8/24	4.52	4.53	0.002	9/30	8.45	8.45	0.000	11/5	11.43	11.43	0.000
7/20	1.45	1.46	0.007	8/25	4.56	4.57	0.002	10/1	8.50	8.49	0.001	11/6	11.48	11.48	0.000
7/21	1.49	1.49	0.000	8/26	4.62	4.62	0.000	10/2	8.58	8.59	0.001	11/7	11.65	11.64	0.010
7/22	1.56	1.56	0.000	8/27	5.03	5.04	0.002	10/3	8.76	8.76	0.000	11/8	11.68	11.67	0.010
7/23	1.61	1.61	0.000	8/28	5.04	5.07	0.006	10/4	8.87	8.86	0.001	11/9	11.70	11.70	0.000
7/24	1.62	1.63	0.006	8/29	5.13	5.12	0.002	10/5	8.89	8.87	0.002	11/10	11.70	11.68	0.020
7/25	1.73	1.73	0.000	8/30	5.23	5.24	0.002	10/6	8.92	8.91	0.001	11/11	11.93	11.95	0.020
7/26	1.81	1.81	0.000	8/31	5.28	5.26	0.004	10/7	9.09	9.07	0.002	11/12	11.98	11.96	0.020
7/27	1.83	1.83	0.000	9/1	5.43	5.44	0.002	10/8	9.16	9.19	0.003	11/13	12.01	12.02	0.010
7/28	1.84	1.84	0.000	9/2	5.65	5.62	0.005	10/9	9.20	9.19	0.001	11/14	12.04	12.05	0.010

7/29	2.27	2.27	0.000	9/3	5.74	5.75	0.002	10/10	9.21	9.22	0.001	11/15	12.04	12.03	0.010
7/30	2.31	2.31	0.000	9/4	6.06	6.06	0.000	10/11	9.22	9.22	0.000	11/16	12.09	12.09	0.000
7/31	2.33	2.32	0.004	9/5	6.20	6.21	0.002	10/12	9.27	9.26	0.001	11/17	12.13	12.13	0.000
8/1	2.37	2.36	0.004	9/6	6.23	6.23	0.000	10/13	9.32	9.33	0.001	11/18	12.43	12.42	0.010
8/2	2.38	2.37	0.004	9/7	6.41	6.39	0.003	10/14	9.43	9.44	0.001	11/19	12.53	12.55	0.020
8/3	2.46	2.45	0.004	9/8	6.43	6.42	0.000	10/15	9.55	9.56	0.001	11/20	12.71	12.70	0.010
8/4	2.47	2.45	0.008	9/9	6.55	6.53	0.000	10/16	9.60	9.59	0.001	11/21	12.71	12.71	0.000
8/5	2.52	2.53	0.004	9/10	6.69	6.70	0.007	10/17	9.67	9.67	0.000	11/22	12.76	12.75	0.010

IV. C. Deformation warning analysis

The displacement-deformation increment parameter is a reflection of geotechnical behavior, and the monitoring value is the deformation increment value, which avoids the deformation error caused by parameter damage. Figure 5 shows the distribution of surrounding rock deformation during the construction process, where (a)~(d) are k=1.6, 1.9, 2.2, 2.5, respectively, and k represents the discount factor. From the figure, it can be seen that the deformation of the top arch and downstream arch base is not obvious, while the deformation of the upstream arch base and the side wall has a larger increase, indicating that this is a part of the enclosing rock that is easy to be destabilized, and the monitoring should be strengthened during the construction process.

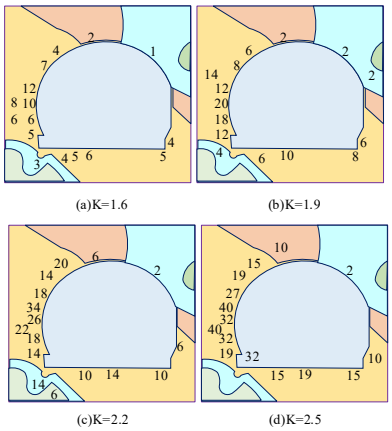

Figure 5: The deformation distribution of surrounding rock in construction process

IV. D. Dynamic monitoring and early warning and engineering regulation

The deformation-time curve of each monitoring point is shown in Fig. 6, in which S1~S4 represent the displacement measurement sensors respectively, and the reading of the sidewall measurement point reaches 32 mm, and the deformation value is larger than that of the sidewall measurement point of the other multi-point displacement meter, close to the warning value of 24 mm obtained by the calculation of this paper, and there is obvious safety hazard in the upstream sidewall enclosure rock. Subsequently, on the basis of the original support program, the field personnel added two rows of 11m long ϕ26mm shell type prestressed hollow grouting anchors for reinforcement, from the monitoring deformation curve can be seen, then the deformation rate of the enclosing rock decreased significantly, and the deformation tends to converge.

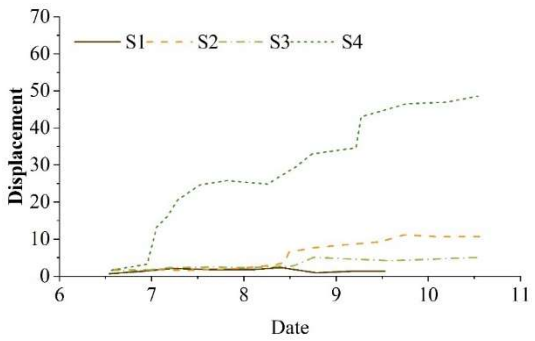

Figure 6: Each monitoring point deformation - time curve

The distribution of principal stresses in the surrounding rock after excavation of the plant is shown in Fig. 7, and the deformation and damage mechanism of the surrounding rock is shown in Fig. 8. After the investigation and analysis by the on-site geologists, the existence of a weak fragmentation zone and unfavorable structural surface combination in the upstream side wall was ruled out. The maximum principal stress of the upstream sidewall is concentrated, while the minimum principal stress is relatively slack, as analyzed by the gross cavern normal calculation (Fig. 7). This unfavorable stress condition makes the upstream side wall easier to be destabilized (Figure 8), which is the reason for the dangerous large deformation of the upstream side wall. Calculating the above engineering examples, the deformation warning value of the surrounding rock is obtained by applying the geotechnical calculation method, and the stability condition of the surrounding rock is analyzed by comparing with the monitoring value. Then, the support scheme was adjusted according to the situation, and the upstream sidewall perimeter rock destabilization was successfully avoided. According to the research line of dynamic early warning, the same deterioration calculation method is used to obtain the deformation warning value of 63mm for the excavation of the 3rd layer to the point D after the excavation, when the excavation of the 3rd layer is completed, the displacement meter monitors the deformation value to be around 45mm, which is smaller than the warning value, and the surrounding rock is always in a stable state, which ensures that the subsequent construction of the excavation is carried out smoothly.

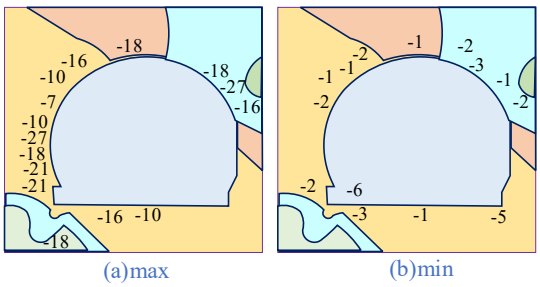

Figure 7: The main stress distribution of surrounding surrounding rock after excavation

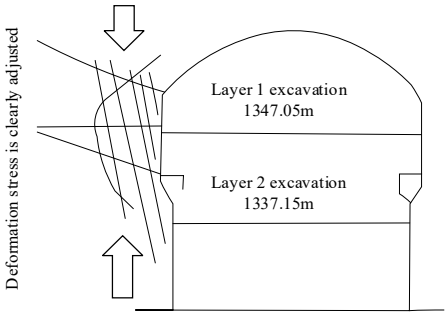

Figure 8: Mechanism of deformation and destruction of surrounding rock

V. Conclusion

In order to understand the geotechnical behavior in the construction of underground engineering, a combination of genetic algorithm and support vector machine is used to construct a model for monitoring the geotechnical behavior in the construction of underground engineering, and the model is validated and analyzed. The research results are as follows:

(1) The relative errors between the results of geotechnical parameter inversion using GA-SVM method and the measured parameters of the project are all within 5%, indicating that the method can obtain the optimized geotechnical parameters for monitoring and data analysis in a relatively simple, economical and accurate way.

(2) In the displacement monitoring of geotechnical behavior, the maximum relative error of prediction reaches 0.083, and the overall displacement prediction error is 0.084%, and the error is within 5%, which confirms that the geotechnical behavior monitoring method based on the optimization of genetic algorithms and support vector machines is practicable.

(3) When the discount factor is taken as 1.6, 1.9, 2.2, 2.5, the deformation change of the top arch and downstream arch base is not obvious the deformation change of the top arch and downstream arch base is not obvious the deformation change of the top arch and downstream arch base is not obvious, on the contrary, while the deformation

increase of the upstream arch base and the side wall is larger, which reacts to the peripheral rock of the underground project is easy to be destabilized parts, and the monitoring should be strengthened in the process of construction.

References

[1] Powrie, W. (2018). Soil mechanics: concepts and applications. CRC Press.

[2] Wang, H., Tian, K., Ma, B., Zhang, H., Zhang, R., & Li, D. (2021). Soil mechanics. Soil Mechanics and Foundation Engineering, 58(2).

[3] Wang, Q., Gao, S., Jiang, B., Li, S., He, M., Gao, H., & Qin, Q. (2018). Rock-cutting mechanics model and its application based on slip-line theory. International Journal of Geomechanics, 18(5), 04018025.

[4] Zou, D. (2017). Theory and technology of rock excavation for civil engineering (p. 699). Singapore: Springer Singapore.

[5] Wei, H. Z., Xu, W. J., Xu, X. F., Meng, Q. S., & Wei, C. F. (2018). Mechanical properties of strongly weathered rock–soil mixtures with different rock block contents. International Journal of Geomechanics, 18(5), 04018026.

[6] Rahimi, B., Sharifzadeh, M., & Feng, X. T. (2021). A comprehensive underground excavation design (CUED) methodology for geotechnical engineering design of deep underground mining and tunneling. International Journal of Rock Mechanics and Mining Sciences, 143, 104684.

[7] Kanji, M. A., He, M., & e Sousa, L. R. (Eds.). (2020). Soft rock mechanics and engineering. Chem, Switzerland: Springer.

[8] Gong, H., Kizil, M. S., Chen, Z., Amanzadeh, M., Yang, B., & Aminossadati, S. M. (2019). Advances in fibre optic based geotechnical monitoring systems for underground excavations. International Journal of Mining Science and Technology, 29(2), 229-238.

[9] Wu, F., Wu, J., Bao, H., Li, B., Shan, Z., & Kong, D. (2021). Advances in statistical mechanics of rock masses and its engineering applications. Journal of Rock Mechanics and Geotechnical Engineering, 13(1), 22-45.

[10] Lawal, A. I., & Kwon, S. (2021). Application of artificial intelligence to rock mechanics: An overview. Journal of Rock Mechanics and Geotechnical Engineering, 13(1), 248-266.

[11] Souček, K., Vavro, M., Staš, L., Vavro, L., Waclawik, P., Konicek, P., ... & Vondrovic, L. (2017). Geotechnical characterization of Bukov underground research facility. Procedia engineering, 191, 711-718.

[12] Lato, M. (2021). Canadian Geotechnical Colloquium: Three-dimensional remote sensing, four-dimensional analysis and visualization in geotechnical engineering—State of the art and outlook. Canadian Geotechnical Journal, 58(8), 1065-1076.

[13] Dingli, Z. (2017). Essential issues and their research progress in tunnel and underground engineering. Chinese Journal of Theoretical and Applied Mechanics, 49(1), 3-21.

[14] Kashani, A. R., Chiong, R., Mirjalili, S., & Gandomi, A. H. (2021). Particle swarm optimization variants for solving geotechnical problems: review and comparative analysis. Archives of Computational Methods in Engineering, 28, 1871-1927.

[15] Wang, D. Y., Li, X. B., Peng, K., Ma, C. D., Zhang, Z. Y., & Liu, X. Q. (2018). Geotechnical characterization of red shale and its indication for ground control in deep underground mining. Journal of Central South University, 25(12), 2979-2991.

[16] Juang, C. H., Zhang, J., Shen, M., & Hu, J. (2019). Probabilistic methods for unified treatment of geotechnical and geological uncertainties in a geotechnical analysis. Engineering geology, 249, 148-161.

[17] Moayedi, H., Mosallanezhad, M., Rashid, A. S. A., Jusoh, W. A. W., & Muazu, M. A. (2020). A systematic review and meta-analysis of artificial neural network application in geotechnical engineering: theory and applications. Neural Computing and Applications, 32, 495-518.

[18] Fernandes, M. M. (2020). Analysis and design of geotechnical structures. CRC Press.

[19] Phoon, K. K., Cao, Z. J., Ji, J., Leung, Y. F., Najjar, S., Shuku, T., ... & Ching, J. (2022). Geotechnical uncertainty, modeling, and decision making. Soils and Foundations, 62(5), 101189.

[20] Zhang, W., Gu, X., Hong, L., Han, L., & Wang, L. (2023). Comprehensive review of machine learning in geotechnical reliability analysis: Algorithms, applications and further challenges. Applied Soft Computing, 136, 110066.

[21] Yang, Z., & Ching, J. (2019). A novel simplified geotechnical reliability analysis method. Applied Mathematical Modelling, 74, 337-349.

[22] Hryhorii Larionov,Volodymyr Sapehin,Yuliia Zemliana,Viktor Khvorostian & Sofiia Holovko. (2024). Method of successive approximation in mathematical modelling of geotechnical mechanics problems.IOP Conference Series: Earth and Environmental Science(1),

[23] Benjamin R Anderson,Andrew O'Kins,Kostiantyn Makrasnov,Rebecca Udby,Patrick Price & Hergen Eilers.(2024).A modular GUI-based program for genetic algorithm-based feedback-assisted wavefront shaping.Journal of Physics: Photonics(4),045008-045008.

[24] W S Mada Sanjaya,Akhmad Roziqin,Agung Wijaya Temiesela,M Fauzi Badru Zaman,Ahsani Taqwim,Intan Opialisti... & Tsamrotus Sa'adah.(2024).Developing an electronic nose for formalin detection in meatballs using Support Vector Machine (SVM) method and Raspberry Pi 4.Physica Scripta(9),096009-096009.